Wave-Coupled LiNbO$_3$ Electro-Optic Modulator for

Microwave and Millimeter-Wave Modulation[*]

William B. Bridges and Finbar T. Sheehy

California Institute of Technology

and

James H. Schaffner

Hughes Research Laboratories

I.   ABSTRACT

The phase velocity mismatch due to material dispersion in traveling-wave LiNbO$_3$ optical waveguide modulators may be greatly reduced by breaking the modulation transmission line into short segments and connecting each segment to its own surface antenna. The array of antennas is then illuminated by the modulation signal at an angle which produces a delay from antenna to antenna to match the optical waveguide's delay.

A phase modulator, 25 mm long with 5 dipole antenna/transmission-line elements, was operated from 4.3 to 13 GHz with a maximum phase modulation sensitivity of about 100 degrees/Watt$^{1/2}$. The optical wavelength was 633 nm. The expected variation of response with illumination angle was confirmed. A simple theory of antenna and transmission-line modulator behavior has been developed that matches the measured frequency response. This work was reported previously [1].

A second phase modulator, 18 mm long with 20 antenna/transmission-line elements, was operated at V-band and had a maximum phase modulation sensitivity of approximately 80 degrees/Watt$^{1/2}$. This showed that the modulator design can be scaled for mm-wave operation quite successfully.

A third modulator, using broad-band bow-tie antennas and designed for the range 60-100 GHz is being fabricated currently. The antenna array has provision for application of a dc bias voltage to the electrodes in order to bias a Mach-Zehnder optical amplitude modulator to the proper operating point.

II.   INTRODUCTION

Electro-optic modulators using $LiNbO_3$ have been demonstrated with modulation frequencies over 17 GHz and with modulation voltages less than 1 V [2,3]. Unfortunately there is a trade-off between sensitivity and bandwidth. While $LiNbO_3$ has a high electro-optic coefficient, it is also dispersive, having a much higher refractive index for microwave frequencies than for optical signals. The consequent mismatch of optical and microwave phase velocities limits the useful interaction length to about one-quarter free-space wavelength at the microwave frequency. If the modulator is long, for high sensitivity, then the maximum modulation frequency is low: if the modulation frequency is high then the modulator must be kept short, limiting sensitivity. We have demonstrated a new technique which overcomes this limitation and, as an added benefit, uses a waveguide to introduce the modulation signal. This latter feature may prove as important as the former for modulators operating in the millimeter wave range.

There have been previous approaches to overcoming the material dispersion limitation so as to achieve high modulation frequencies. Alferness et al.[4] have demonstrated a technique in which the modulation electrodes are divided into sections, each of which introduces a phase error of 180° between the optical and modulating signals. The sections are then connected together so as to correct the phase by 180°. In this way the average phase velocities of the two signals are kept equal. Some loss of sensitivity does occur because the electrode length which is required to introduce the 180° phase error is quite long.

Schaffner[5] has divided the electrodes into shorter sections to obtain greater sensitivity. The sections are connected by stub transmission lines that provide a phase delay of 360° minus the phase error introduced by each short electrode section. As in reference 4, the average phase velocity of the modulating signal is kept equal to that of the optical signal, but the shorter sections improve the sensitivity. However, as the sensitivity is increased by adding more sections, the bandwidth about the design frequency is decreased. This is also true of the Alferness method.

Our technique also divides the modulator into sections which limit the phase error per section. Now the individual sections are connected to surface antennas, as shown in Figure 1. The antennas are illuminated by a plane wave (the modulating signal) at an angle which provides the required phase-shift between modulator elements. Since the $LiNbO_3$ has a high value of ϵ_r the antennas are much more sensitive to radiation incident from inside the substrate than from outside [6]. The required angle of incidence for the plane-wave illumination is $\theta = \sin^{-1}(n_o/n_m)$ where n_o is the optical refractive index and n_m is the microwave refractive index of $LiNbO_3$. The addition of more modulator sections

does not affect the bandwidth in this case, as the bandwidth is simply that of a single modulator element.
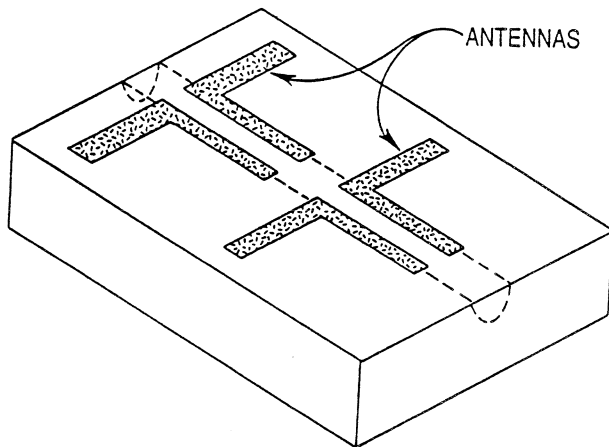

Figure 1. Schematic drawing of two dipole antennas and connected transmission line sections on the surface of a waveguide E-O modulator.

Since no physical connections are made to the antennas and the short modulating elements need not be terminated by matched loads (although they could be), no parasitic circuit elements (such as bond wires or connectors) are introduced which might limit the possibility of scaling to higher frequencies. The limits would be imposed by the size of the optical waveguide and by the absorbtion spectrum of the $LiNbO_3$ itself [7]. A modulator at 500 GHz should be quite practical (Figure 2). In addition, at these very high frequencies the attenuation per unit length in the modulating electrodes can be very high. In the antenna-coupled modulator the problem of attenuation of the modulating signal as it propagates from section to section does not exist, since the elements are driven "from the side", in parallel rather than in series. Since the number of modulator sections required would be large, the antenna-coupled modulator's bandwidth advantage becomes important also. In exchange for these advantages, we must develop efficient means for illuminating the modulator.
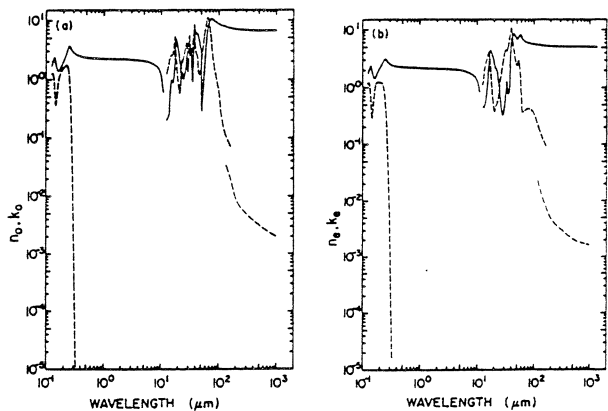

Fig. 7. (a) Log–log plot of n, (——) and k, (----) versus wavelength in micrometers for lithium niobate. (b) Log–log plot of n, (——) and k, (----) versus wavelength in micrometers for lithium niobate.
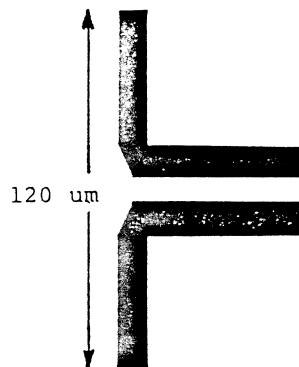
120 um

Figure 2. The absorbtion spectrum of $LiNbO_3$ and scaling of modulator elements show that a 500 GHz modulator is feasible.

III.   X-BAND PROTOTYPE MODULATOR

Figure 3 shows the mask for an X-band prototype modulator. There are five antenna/modulator sections. The overall length is 25 mm. The antennas are "two half-waves in phase" dipoles, and the modulator sections are approximately a half-wave long at 12 GHz, based on an assumed effective microwave surface refractive index of 3.8 (i.e. the dielectric constant is taken as the mean of the dielectric constants of air and $LiNbO_3$). This electrode pattern was positioned over a straight section of optical waveguide to produce a phase modulator rather than a Mach-Zehnder amplitude modulator, but the same mask would also work if applied to one arm of a Mach-Zehnder. The 6μm optical waveguide was produced by in-diffusion of titanium.
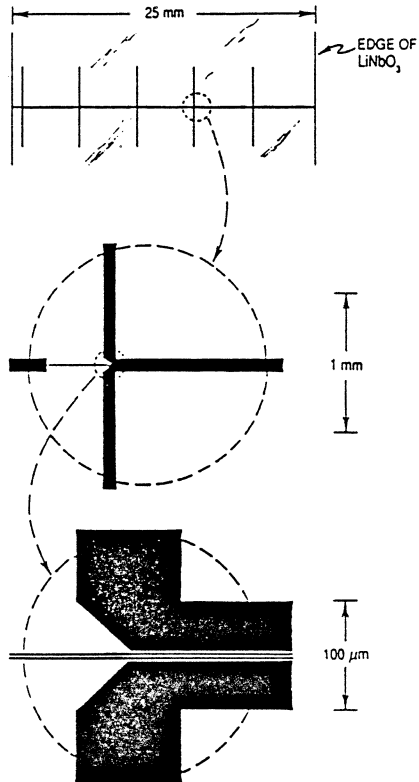
Figure 3. Photolithographic mask for 5 antenna-plus-transmission lines covering a 25 mm long optical waveguide. Magnified details are shown in the lower two drawings.

The microwave feed used to drive the modulator is shown in Figure 4. The $LiNbO_3$ substrate is attached to a wedge of Stycast [R] dielectric with $\epsilon_r=30$, and the signal is matched into this material by two matching layers of intermediate dielectric constant. The wedge angle is $23°$ to match the microwave and optical phase velocities: a wedge is necessary because the critical angle is only $9°$, making it impossible to couple into a flat substrate at any larger angle. The optical beam is coupled into and out of the optical waveguide using microscope objectives. Optical damage occurs in the guide at the 633 nm optical wavelength used, and optical power was limited because of this.

As was mentioned above, the pattern of an antenna on a dielectric substrate is directed more into the substrate than into the air. For $\epsilon_r=30$ there is virtually no coupling on the air side. The pattern
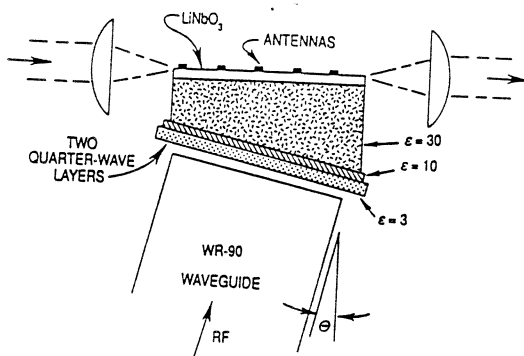
Figure 4. Schematic side view of an experimental modulator

showing $LiNbO_3$ wafer with antennas, input and output

lenses, wedged block of high dielectric constant material,

matching layers, and microwave waveguide.

in the dielectric is also distorted by the presence of the interface. There is a peak response in the direction of the critical angle (here 9°). We used the theory of Enghetta et al. [4] to evaluate the pattern at the desired angle of 23°, and find that it is only about 0.5 dB down from the peak (Fig. 5).
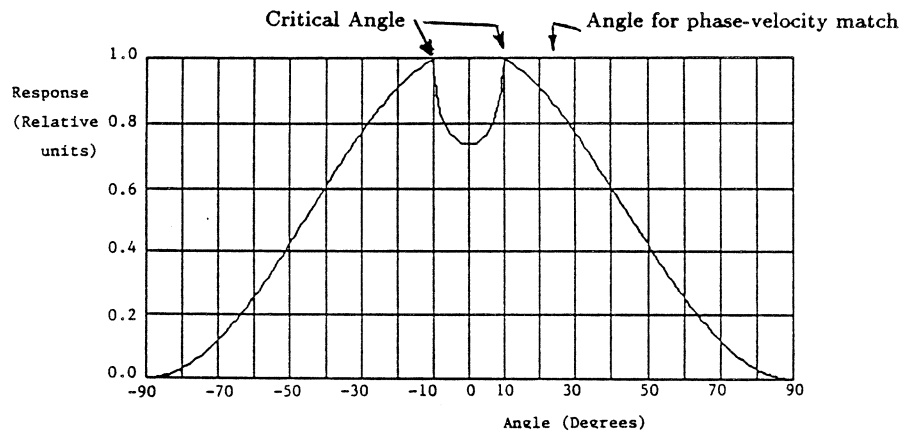

Figure 5. Antenna pattern of Dipole on $LiNbO_3$. (The cusp-like behavior at the critical angle is a real feature.)

The phase modulated signal cannot be detected using an amplitude detector. We used a scanning Fabry-Perot interferometer to show the existence of modulation sidebands and measure their amplitude. The phase deviation introduced by the modulator can be deduced from the amplitude of the sidebands relative to the carrier (for small phase deviation) from the formula [8]

$$\Delta\phi = 2 \sqrt{\frac{P_{sideband}}{P_{carrier}}}$$

It is more usual to build an amplitude modulator and detect the signal directly, but the above method is simple and has the advantage that it works at much higher modulation frequencies, where a-m detectors are scarce. It has one notable disadvantage, however. The frequency spectrum is aliased by the scanning Fabry-Perot at frequency intervals equal to the free spectral range, so that sidebands which are an integral number of free spectral ranges off carrier are lost behind an aliased version of the carrier.

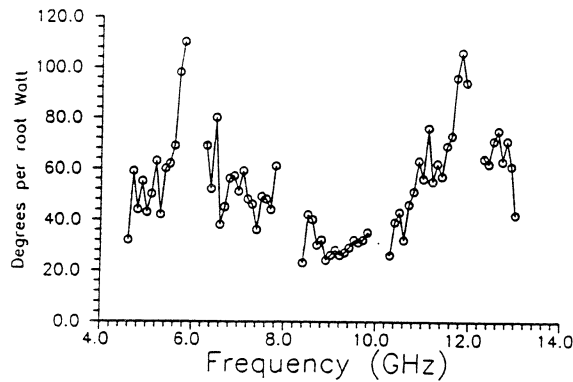Figure 6 shows the modulator response as a function of frequency. The response is here defined as phase deviation normalized to the square root of the drive power, in units of "degrees per root Watt". This measure is linearly related to "degrees/radians per Volt", which is the common measurement when direct connections are made and voltage can be measured directly. There are no data points at 6, 8, 10 and 12 GHz due to the aliasing of the carrier at 2 GHz intervals making the sidebands invisible on the oscilloscope display. The graph shows straight-line interpolation between the data points.

Figure 6. Frequency response of the experimental X-band modulator.

The modulator was operated with a number of different wedge angles to establish the effect of the illumination angle on performance. This may be modeled by considering the pattern of each antenna alone, the pattern of a phased array of such antennas (with the light in the optical waveguide doing the phasing), and the pattern of a phased array of antennas with unequal illumination. Figure 7 shows the patterns of arrays of 3, 4 and 5 equally illuminated an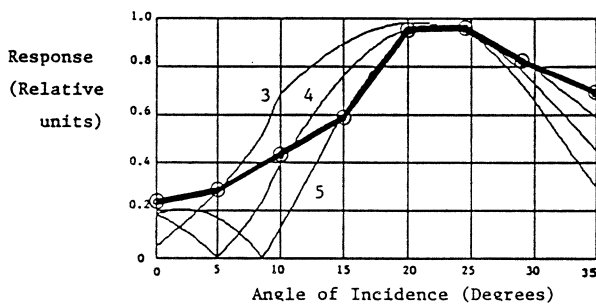tennas. We have included the smaller numbers of antennas because the antennas at either end of the modulator may be poorly illuminated. If a cosine distribution across the five antennas is assumed, the result is not unlike the 4-antenna case. Also plotted in Figure 7 is the average response over the 9-12 GHz band of the prototype modulator at each angle of incidence. The response peaks at about 23° as expected, confirming the phase-velocity-matching picture. The absence of the null in the experimental data is probably due to the multiple reflections inside the wedge.

Figure 7. Effect of illumination angle on performance: theory for 3,4, and 5 antennas, and results from experimental modulator.

IV. V-BAND PROTOTYPE MODULATOR

A V-band phase modulator was designed based on scaling of the X-band prototype. The mask is shown in Figure 8. Essentially the design 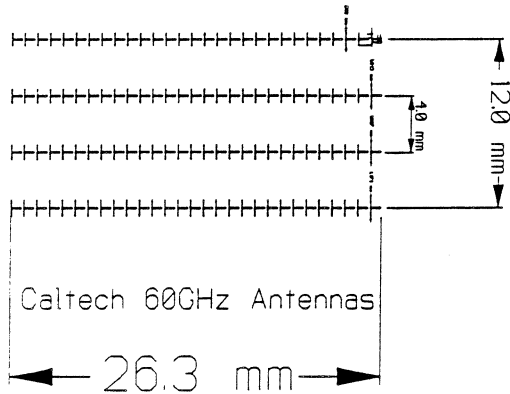of each antenna/modulator element is based on a direct scaling of the original prototype, except that the electrode gap dimensions are fixed, and this fixes the lateral dimensions of the electrodes.

Since the mm-wave waveguide from which the modulating signal originates is now much smaller, while the antenna array is still long (more antennas), a different microwave feed is needed. The modulating signal is coupled from the waveguide into a tapered slab waveguide 1.5 mm thick. This tapered slab provides

Figure 8. V-Band Modulator mask.

a means of expanding the wave to the dimensions of the antenna array, which was 1 x 18 mm. The power is matched into a slab of LiNbO$_3$ which is cut as a wedge to provide the correct angle of incidence for the modulating signal. The microwave feed is shown in Figure 9.
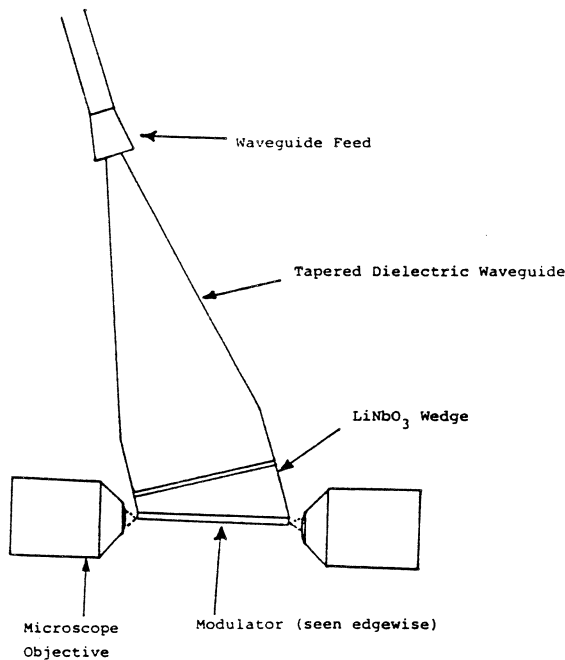
The phase deviation was again measured using the scanning Fabry-Perot method, which works just as well with mm-wave as with microwave modulation. However we did not have complete confidence in the accuracy of our V-band power meter, and so can give only approximate results in terms of degrees of phase deviation per Watt$^{1/2}$. These results are shown in Figure 10.
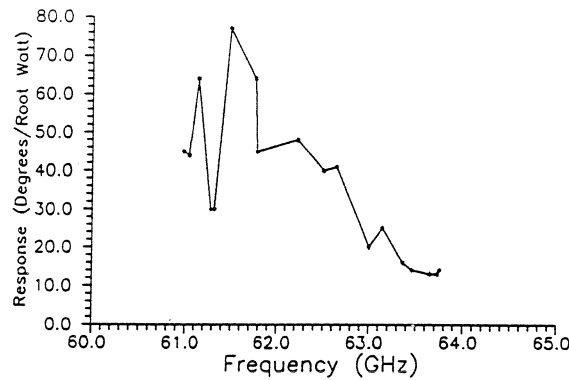
Figure 9. The V-band microwave feed.

Figure 10. Frequency Response of the V-band

prototype modulator.

V. DISCUSSION OF RESULTS

The structure of the frequency response arises from many sources: antenna and electrode resonance; reflections within the wedge; nonideal input matching layers; etc. However, we have found that the general shape of the X-band prototype modulator response is accounted for quite well by a model of the antenna/electrode impedance variations and the frequency response of the individual modulators. In this model the electrodes are treated as lossless transmission lines, open-circuit at the end; the antenna is treated as a lossy transmission line (the loss represents radiation effects); and the individual modulators have a frequency response basically determined by the well-known sinc-function response, except that there are two sinc terms, one for the forward-propagating wave at the modulation frequency and one for the wave reflected back from the open circuit at the end of the modulator electrodes.

The frequency response which is predicted by this simple model of impedances, modulator element frequency response and antenna gain is shown in Figure 11. It agrees remarkably well with the general shape of the experimentally determined response of the X-band prototype.
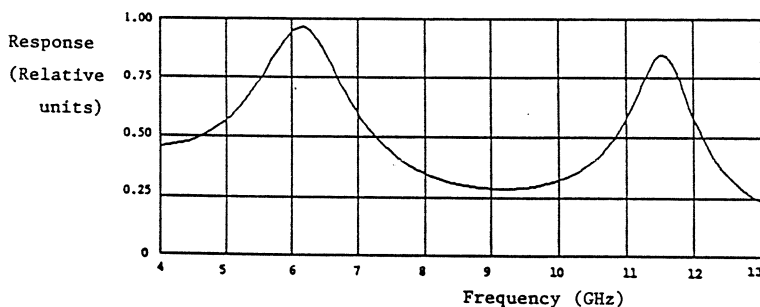

Figure 11. Frequency response predicted by simple model of antenna and electrode impedances, modulator element frequency response and antenna gain.

The peak around 12 GHz occurs when the modulator elements are a half wave long, at which point the antennas are approximately two half-wavelengths long. The antenna driving-point impedance and the modulator element input impedance are then both high. At 6 GHz there is another peak when the antenna is a half-wave long and the modulator element has a low input impedance. The lower-frequency peak also benefits from the increased modulator sensitivity at lower frequency - the modulator electrodes are electrically shorter and the sinc terms are nearer to unity. It was necessary to use WR 137 waveguide to measure this lower-frequency peak, so the microwave feed geometry was changed.

Peak response values exceed 100 degrees per $W^{1/2}$. This compares favorably with conventional microwave modulators (Erasme et al.[9] report a peak response of 131 degrees per $W^{1/2}$ for their phase-reversal travelling-wave modulator, operating at a wavelength of 1153 nm - note that sensitivity varies as $1/\lambda_{optical}$). This is only achieved over a narrow band, but is encouraging in a prototype. The narrow bandwidth results from the use of simple resonant elements. Other antenna designs with broadband elements will likely result in a flatter frequency response. Of course even here there is a region between the two peaks which is quite flat, but less sensitive by about 10 dB.

VI. FUTURE DEVELOPMENTS

To date we have demonstrated that the antenna-coupled modulator is capable of efficient mm-wave modulation of optical signals. However, the structure used had a relatively narrow bandwidth and was not ideally suited for use as part of a Mach-Zehnder amplitude-modulator structure. The Mach-Zehnder design requires a DC bias to ensure that the modulation drives the interferometer in its most linear (and most sensitive) regime. There is no good way to connect DC bias leads to the surface dipoles. A new modulator has been designed to overcome these two difficulties and is being fabricated at present. This new modulator uses bow-tie antennas in place of the dipoles. The bow-ties approximate frequency-independent structures, and this should allow much greater bandwidths. In addition the ends of the bow-ties interact only weakly with the radiation field and can be used as bias leads with little effect on RF performance. There is some sensitivity penalty associated with the use of these antennas, since the peaking of the response which was due to the dipole resonances is lost. The new modulator is designed to operate as a Mach-Zehnder amplitude modulator over the range 60-94 GHz. We also propose to demonstrate operation at 1.3 μm and/or 1.5 μm optical wavelengths.

The theory of antennas on dielectric substrates is not very well developed, although dipoles are well understood. Further developments in this area will be applicable to these modulators. Improved waveguide-to-antenna coupling is also desireable. Demonstrations at significantly higher modulation

frequencies would depend very much on the availability of mm-wave or sub-mm-wave power sources.

VII. ACKNOWLEDGEMENTS

The authors wish to acknowledge the technical support of Robert L. Joyce and Reynold E. Johnson in this work, and many valuable discussions with Robert W. Terhune.

VIII. REFERENCES

[1]   William B. Bridges, F. T. Sheehy, and James H. Schaffner, "Velocity-Matched Electro-Optic Modulator," SPIE Vol. 1371 High Frequency Analog Fiber Optic Systems (1990) pp. 68-77, San Jose, California, September 1990

[2]   G. E. Betts, L. M. Johnson, and C. H. Cox, III, "High-Sensitivity Lumped-Element Bandpass Modulators in $LiNbO_3$," IEEE J. Lightwave Tech., Vol. 7, pp 2078-2083, December 1989.

[3]   C. M. Gee, G. D. Thurmond, and H. W. Yen, "17-GHz Bandwidth Electro-Optic Modulator," Appl. Phys. Lett., Vol. 43, pp 998-1000, December 1983.

[4]   R. C. Alferness, S. K. Korotky, and E. A. J. Marcatili, "Velocity-Matching Techniques for Integrated Optic Traveling Wave Switch/Modulators," IEEE J. Quant. Electron., Vol. QE-20, pp 301-309, March 1984.

[5]   J. H. Schaffner, "Analysis of a Millimeter Wave Integrated Electro-optic Modulator with a Periodic Electrode," Paper 13 at SPIE OE-LASE Conference 1217, Proceedings, pp 101-110, Los Angeles, Calif., January 16-17, 1990.

[6]   N. Enghetta, C. H. Papas, and C. Elachi, "Radiation Patterns of Interfacial Dipole Antennas," Radio Science, Vol. 17, pp 1557-1566, Nov.-Dec. 1982.

[7]   Handbook of Optical Constants of Solids, Edward D. Palik, Academic Press 1985

[8]   See, for example, Reference Data for Radio Engineers, 5th Ed., Howard Sams, New York, 1968, Sec. 21-7.

[9]   D. Erasme, D. A. Humphries, A. G. Roddie, and M. G. F. Wilson, "Design and Performance of Phase Reversal Traveling Wave Modulators," IEEE J. Lightwave Tech., Vol. 6, pp 933-936, June 1988.